International Journal of Advanced Technology and Innovative Research

www.ijatir.org

ISSN 2348–2370
Vol.08,Issue.12,
September-2016,
Pages:2351-2357

A Low Multiplicity Composition of PAPR Degradation in OFDM Systems with Near-Optimal Performance

S. PAVANI[1], DR. C. SUBHAS[2]

[1]PG Scholar, Sree Vidyanikethan Engineering College, A.Rangampet, Tirupathi, AP, India.

[2] Professor and Dean of Academics, Sree Vidyanikethan Engineering College, A.Rangampet, Tirupathi, AP, India.

Abstract: To reduce the PAPR in OFDM systems selected mapping schemes (SLM) are widely used due its distortion less nature. However a major drawback of traditional SLM technique is high computational complexity to select a low PAPR signal it requires a bank of inverse fast Fourier (IFFT) operations. This paper proposes a novel architecture for PAPR reduction in OFDMs with low computational complexity. In this proposed method, frequency domain cyclic shifting, complex conjugate, sub-carrier reversal operations are performed to increase the PAPR reduction performance in OFDM systems whereas in traditional SLM scheme only frequency domain phase rotation can be performed to generate the candidate signals. Furthermore, to reduce the multiple IFFT problems, all of the frequency domain equivalent operations are converted into time-domain equivalents. It is shown that the sub carrier partitioning and re-assembling processes are important in realizing low complexity time domain equivalent operations. Moreover, it is shown theoretically and numerically that the computational complexity of the proposed scheme is significantly lower than the traditional SLM method and the PAPR reduction performance is within 0.001 dB of that SLM.

Keywords: Orthogonal Frequency Division Multiplexing (OFDM), Peak to Average Power Ratio(PAPR), Selected Mapping Scheme (SLM).

I. INTRODUCTION

After more than thirty years of research and development, OFDM has been extensively adapted in wireless communications due to its low vulnerability to multipath propagation and high spectral efficiency. In many applications, high data rate transmissions are required over wireless channels with OFDM systems. However a major drawback of OFDM based transmission system is its high PAPR, which leads to in-band distortion and out of band radiation when the signals are passed through a non-linear power amplifier. There are various proposals for PAPR reduction in OFDM systems in literature, including tone reservation,tone injection, clipping, partial transmit sequence, activeconstellation extension, nonlinear companding, selected mapping(SLM). Among all these techniques SLM is most commonly used due to its distortion less nature. However a major drawback of traditional SLM technique is high computational complexity to select a low PAPR signal it requires a bank of inverse fast Fourier (IFFT) operations. To reduce the computational complexity, several low-complexity SLM architectures have been proposed [14]-[16] in which the frequency domain phase rotations are converted into equivalent frequency domain phase rotations. This paper proposes a novel architecture for PAPR reduction in OFDMs with low computational complexity. In this proposed method, frequency domain cyclic shifting, complex conjugate, sub-carrier reversal operations are performed to increase the PAPR diversity in OFDM systems whereas in traditional SLM scheme only frequency domain phase rotation is used to generate the candidate signals.

II. MODEL OF A SYSTEM

Consider an OFDM system with N-subcarriers. Let the modulated symbols form an $N \times 1$ frequency domain data vectors is given by,

$$X = [X[0], X[1], \dots\dots\dots\dots, X[N-1]]^T,$$

where X[K] denotes the modulated symbol of the K^{th} sub-carrier and $(\cdot)^T$ is transpose operation. An $N-$point operation of time domain signal vector of x is given by

$$x[n] = \frac{1}{\sqrt{N}} \sum_{k=0}^{N-1} X[K].\exp\left\{\frac{j2\pi nk}{N}\right\}, \quad n = 0,1,2, \dots\dots, N-1 \tag{1}$$

The PAPR of the discrete time OFDM signal is given by,

$$PAPR(X) = \frac{\max\limits_{0 \le n \le N-1} |x[n]|^2}{E[|x[n]|^2]} \tag{2}$$

Where E[·] denotes expectation operation. For OFDM systems generally complementary cumulative distribution function is used to evaluate the PAPR reduction performance. The CCDF is used to measure the probability that the PAPR of a certain data block exceeds the given threshold γ i.e. ,

$$CCDF_{PAPR(X)} = Pr(PAPR(X) > \gamma) \tag{3}$$

III. PAPR REDUCTION OF OFDM SYSTEMS IN FREQUENCY DOMAIN

This section describes the implementation of PAPR reduction in OFDM systems in frequency domain. In this

scheme, the PAPR diversity of the candidate signals is increased by performing frequency domain cyclic shift complex conjugate, subcarrier reversal operations whereas in traditional SLM scheme, the candidate signals are generated by performing frequency domain phase rotation only. Consider an OFDM system with N subcarriers. Let the N subcarriers are partitioned into S subcarriers sets $\Gamma_s, s = o, 1, \ldots\ldots\ldots, S-1$. Generally, there are three method for partitioning the subcarriers in OFDM systems namely, localized partitioning method (LPM), distributed partitioning method (DPM), hybrid partitioning method (HPM). In LPM each sub-carrier set consists of a number of adjacent and consecutive sub carriers. Meanwhile, in DPM each sub carrier set consists of a multiple interleaved subcarriers with equal spacing. Finally in HPM the subcarriers are first partitioned into U localized subcarriers sets and those subcarriers are further partitioned into V distributed subcarrier sets. It should be noted that all the frequency domain operations described in the following are performed at the subcarrier set level i.e., X_s. Fig. 1 presents a block diagram of the proposed PAPR reduction scheme in the frequency domain, where the frequency domain data vector X is partitioned into S N ×1 data vectors X_s, s = 0, 1, . . . , S − 1.It is noted that in order to allow the maximum flexibility in partitioning the sub-carrier, the sub-carriers are partitioned using the HPM method. As shown in Fig.1, the S data vectors $X_s, s = 0,1, \ldots, S-1$ are processed by multiple candidate signal generating blocks (CSGBs) in order to generate the candidate signals.

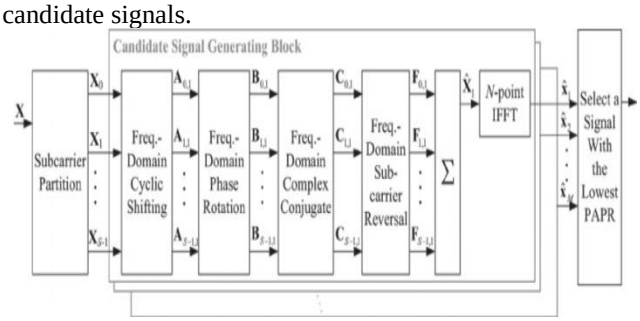

Fig. 1. System architecture of proposed scheme in frequency domain.

(Note that each CSGB generates a single candidate signal.) For illustration purposes, consider the m^{th} CSGB in Fig.1. The first block in the CSGB performs a frequency-domain cyclic shifting operation. Assuming that $l_{s,m}$ cyclic shifts are performed on X_s, the output signal is denoted as $A_{s,m}, s = 0,1, \ldots, S-1, m = 1,2, \ldots, M-1$. Therefore, the k^{th} element of $A_{s,m}$ is given by

$$A_{s,m}[k] = X_s\left[(k - l_{s,m})_N\right] \quad \textbf{(4)}$$

$k = 0,1, \ldots\ldots\ldots, N-1$

Where $(\cdot)_N$ denotes the modulo N operation. Note that the selection of the cyclic shift value $l_{s,m}$ for a given m is not arbitrary, but is jointly considered over various s since different sub-carrier sets cannot occupy the same sub-carrier after the cyclic shifting operation. The second block of the CSGB performs phase rotation in frequency domain. The output of the S^{th} subcarrier set for the m^{th} CSGB is denoted as $B_{s,m}$, with the k^{th} element is given by

$$B_{s,m}[k] = \theta_{s,m}[k] \,.\, A_{s,m}[k] \quad \textbf{(5)}$$

$k = 0,1, \ldots\ldots\ldots, N-1,$

where $\theta_{s,m}[k]$ is a complex number with a unit magnitude.

The third block of the CSGB performs a frequency-domain conjugate operation and the output signal is denoted by $C_{s,m}$. Each subcarrier set chooses arbitrarily whether to perform or not to perform the conjugate operation, in order to generate candidate signals with an uncorrelated PAPR.

$$C_{s,m}[k] = B_{s,m}[k] \quad \text{or} \quad C_{s,m}[k] = B^*_{s,m}[k], \forall k \in \Gamma_s \quad \textbf{(6)}$$

where $*$ denotes the complex conjugate operation.

The fourth block of the CSGB performs a sub-carrier reversal operation in frequency domain on the sub-carrier sets, i.e., the output signal is given by

$$F_{s,m}[k] = C_{s,m}[(-k)_N], \forall\, k \in \Gamma_s \quad \textbf{(7)}$$

The choice of whether or not to perform the reversal operation is not arbitrary, but is jointly considered since different subcarrier sets cannot occupy the same sub-carriers after the subcarrier reversal process. Notably, as for the conjugate operation, each sub-carrier set may or may not choose to perform sub-carrier reversal. Finally, the mth candidate signal in the frequency domain is obtained by summing up the sub-carrier sets of the corresponding CSGB, i.e.,

$$\hat{X}_m = \sum_{s=0}^{S-1} F_{s,m} \quad \textbf{(8)}$$

The candidate signal in the time domain, i.e., $\hat{X}_m$ is obtained by performing an IFFT operation on $\hat{X}_m$. Among all the generated candidate signals, the signal with lowest PAPR is selected for transmission. The above scheme requires MIFFT operations. As a result, the computational complexity of the proposed scheme is extremely high. Theoretically, this problem can be avoided by converting all four frequency-domain operations into time-domain equivalents. However, by simply considering the corresponding IFFT, the conversion process cannot be performed since the time-domain operations should also have a low computational complexity. Thus, in the following section, a more computationally-efficient approach is proposed.

IV. TIME DOMAIN EQUIVALENT PROPERTIES OF OFDM SYSTEMS

In this section, in order to reduce the computational complexity of the frequency domain architecture all four frequency domain operations are converted into equivalent time domain operations. In addition, a time-domain repetition property is introduced in order to further reduce the computational complexity. Note that all

of the operations described in this section (both frequency-domain and time domain) are performed on the sub-carriers of the same set.

Property1: Frequency-Domain Cyclic Shifting/Time Domain Phase Rotation

Performing cyclic shifting on the frequency-domain data vector X is equivalent to performing phase rotation on the corresponding time-domain data vector x, i.e.,

$$F^{-1}\{X[(k-l)_N]\} = x[n].exp\left\{\frac{j2\pi nl}{N}\right\}, \quad (9)$$

Where $F^{-1}[\cdot]$ denotes the IFFT operation, and l is the number of frequency-domain cyclic shifts. Note that for $l \in \{0, \frac{N}{4}, \frac{N}{2}, \frac{3N}{4}\}$, we have $exp\left\{\frac{2\pi jnl}{N}\right\} \in \{\pm 1, \pm j\}$ and the time-domain equivalent operation on the right hand side of (8) does not require any complex multiplications or additions Note also that the choice of cyclic shifts l is not arbitrary.

Property 2: Frequency-Domain Phase Rotation / Time-Domain Cyclic Shifting

Performing phase rotation on the frequency-domain data vector X is equivalent to performing cyclic shifting on the corresponding time-domain data vector x, i.e

$$F^{-1}\left\{X[k].exp\left\{\frac{-j2\pi k\omega}{N}\right\}\right\} = x[(n-\omega)_N], \quad (10)$$

$\omega = 0,1, \ldots\ldots\ldots, N-1$

Property3: Frequency-Domain Complex Conjugate Time-Domain Complex Conjugate of Time-Reversed Signals

Performing the frequency-domain complex conjugate operation is equivalent to performing the complex conjugate operation on the time-reversed signals, i.e.,

$$F^{-1}\{X^*[k]\} = x^*[(-n)_N] \quad (11)$$

Property4:Frequency-Domain Sub-carrier Reversal/Time -Domain Signal Reversal

Performing sub-carrier reversal on the frequency-domain data vector X is equivalent to performing time-domain reversal operation on data vector x, i.e.,

$$F^{-1}\{X[(-k)_N]\} = x[(-n)_N] \quad (12)$$

It should be noted that the frequency-domain sub-carrier reversal operation cannot be performed on arbitrary sub-carrier sets since this may result in different sub-carrier sets occupying the same sub-carriers. Thus, a number of remarks are given in the following to clarify the applicability of the subcarrier reversal operation for the three sub-carrier partitioning methods.

Property 5: Time-Domain Repetition

In DPM, the frequency-domain sub-carriers of any set $\Gamma_s$have an equal spacing S. Consequently, the time-domain signal vector $X_s$has the following repetition characteristic**:**

$$X_s = [X_s^{(0)} \quad \beta_{s,1}X_s^{(0)} \quad \beta_{s,2}X_s^{(0)} \quad \ldots \quad \beta_{s,S-1}X_s^{(0)}]^T \quad (13)$$

where x(0) s is a $1 \times \frac{N}{S}$ vector consisting of the first $\frac{N}{S}$ elements of $X_s, \beta_{s,i} = exp\left\{j2\pi i.\frac{s}{S}\right\}, i = 1,2, \ldots\ldots\ldots, S-1$, It is noted that $\beta_{s,i} \in \{\pm 1, \pm j\}, S = 2,4$.

Furthermore, in HPM, the sub-carriers have an equal spacing of V. Thus, the following property can be obtained:

$$X_s = [X_s^{(0)} \quad \beta_{s,1}X_s^{(0)} \quad \beta_{s,2}X_s^{(''0)} \quad \ldots \quad \beta_{s,V-1}X_s^{(0)}]^T \quad (14)$$

Where $X_s^{(0)}$ is a $1 \times \frac{N}{S}$ vector consisting of first $\frac{N}{V}$ elements of X_s,

$\beta_{s,i'} = exp\left\{j2\pi i'.\frac{s}{V}\right\}, i' = 1,2, \ldots\ldots\ldots, V-1, \beta_{s,i'} \in \{\pm 1, \pm j\}$.

V. PROPOSED PAPR REDUCTION OF OFDM SYSTEMS IN TIME DOMAIN

The above Section has described the implementation of the proposed PAPR reduction scheme in the frequency-domain. However, as discussed, for each generation of a candidate signal it requires an N-point IFFT operation. If the generation of candidate signals increases the number of N-point operations increases and it results as a high computational complexity scheme. To resolve the problem of high computational complexity, this section utilizes the time-domain equivalent operations to construct a low-complexity architecture for PAPR reduction. Fig.2 presents a block diagram of the proposed architecture, in which the frequency-domain data vector X is partitioned into S data vectors X_s of size N×1, s = 0, 1, . . . , S−1. Note that in implementing the proposed architecture, the HPM sub-carrier partitioning method is adopted in order to maximize the PAPR diversity. As shown in Fig. 2, having partitioned the sub-carriers, an IFFT operation is performed X_s on to obtain the corresponding time-domain data vector X_s of size N × 1. It is noted that although the proposed scheme still requires S N-point IFFT operations, the computational complexity of the proposed architecture is much lower than that of the traditional SLM scheme since S is much smaller than the number of candidate signals M. Furthermore, the computational complexity of each N-point IFFT is significantly decreased in the proposed scheme since most of the elements of X_s are zero.

Following the IFFT operations, the time-domain data vectors X_s, s = 0, 1, . . . , S − 1, are processed by M CSGBs in order to generate M candidate signals. It is noted that the summation of X_s generates the original time-domain transmitted signal. In each of the M CSGBs, each X_s is first processed by the time-domain phase rotation block (i.e., the time-domain equivalent of the frequency-domain cyclic shifting operation). The resulting output signal is denoted as$a_{s,m}$, where the nth element is given by

$$a_{s,m}[n] = X_s[n].exp\left\{\frac{j2\pi n.\, l_{s,m}}{N}\right\}, \quad (15)$$

$n = 0,1, \ldots\ldots, N-1$

in which $X_s[n]$ is the nth element of X_s and $l_{s,m}$ is the number of frequency-domain cyclic shifts of Γ_s for the mth candidate signal. The second block of the CSGB performs a time domain cyclic shifting operation, i.e., the time-domain equivalent of the frequency-domain phase

rotation operation. Therefore, the n[th] element of the output signal $b_{s,m}$ has the form of

$$b_{s,m}[n] = a_s\left[(n-\omega_{s,m})_N\right] \quad n = 0,1,\ldots\ldots,N-1 \tag{16}$$

Where $\omega_{s,m}$ denotes the number of cyclic shifts of the s[th] sub-carrier set for the m[th] CSGB. It will be recalled that the frequency-domain phase rotation operation is not arbitrary. In practice, phase rotation is not completely random, and thus the PAPR reduction performance is slightly degraded. However, this drawback is minor compared to the substantial reduction achieved in the computational complexity of the proposed scheme.

The third block in Fig.2 performs the time-domain complex conjugate operation, i.e., the equivalent operation of the frequency-domain complex conjugate process. Since the system arbitrarily chooses whether or not to perform the complex conjugate operation, the nth element of the output signal $C_{s,m}$ has the form

$$c_{s,m}[n] = b_{s,m}[n] \quad or \quad b^*_{s,m}[(-n)_N] \tag{17}$$

As discussed in Section III (Property 4), the sub-carrier sets must be properly re-assembled before performing the time domain signal reversal operation. In particular, when using the HPM partitioning method, the sub-carrier sets must be reassembled in such a way that the partition is equivalent to that obtained using DPM (Remark 3).

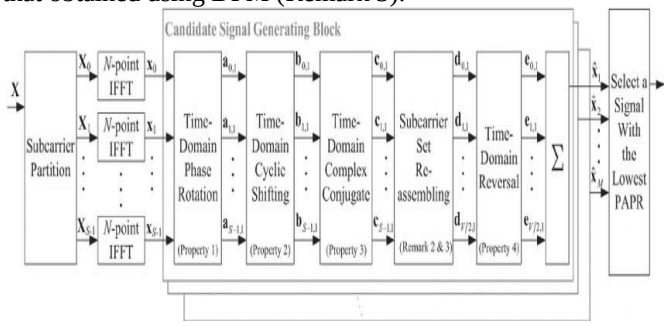

Fig. 2. System architecture of proposed scheme in time domain.

Furthermore, for the case of DPM, the time-domain signal reversal operation can be applied on either $\Gamma_{s=0}\ or\ \Gamma_{s=S/2}$ individually, but should be performed on $\Gamma_s and\ \Gamma_{s-S}$ simultaneously, $s = 1,2,\ldots\ldots,\frac{S}{2}-1$ in order to avoid sub-carrier overlaps (Remark 2). Therefore, the fourth block of the time-domain CSGB performs a subcarrier set re-assembling function, which consists of the two steps. In the first step, the S HPM sub-carrier sets $\Gamma_s, s = 0,1,\ldots\ldots,S-1$ $(S = U.V)$, are combined to obtain the V DPM subcarrier sets $\bar{\Gamma}_{\bar{s}}, \bar{s} = 0,1,\ldots..V-1$ .The $\bar{s}th$ DPM sub-carrier set is obtained by combining the outputs of time-domain complex conjugate operations $c_{(u.v+\bar{s}),m}$, $u = 0,1,\ldots\ldots U-1$ i.e.,

$$\bar{C}_{\bar{s},m} = \sum_{u=0}^{U-1} C_{(u.v+\bar{s}),m}\ ,\quad \bar{s} = o,1,\ldots.,V-1 \tag{18}$$

In the second step, sub-carrier sets are $\bar{\Gamma}_{\bar{s}}\ and\ \bar{\Gamma}_{S-\bar{s}}$, $\bar{s} = 0,1,\ldots\ldots.,\frac{V}{2}-1$ are combined to form a single sub carrier set $\breve{\Gamma}_q$, $q = 0,1,2,\ldots.,\frac{V}{2}-1$, while leaving $\bar{\Gamma}_{\bar{s}=0}\ and\ \bar{\Gamma}_{\bar{s}=V/2}$ unchanged i.e.,

$$d_{q,m} = \begin{cases} \bar{C}_{0,m}, & q = 0, \\ \bar{C}_{\frac{V}{2},m}, & q = \frac{V}{2}, \\ \bar{C}_{q,m} + \bar{C}_{V-q,m}, & q = 1,2,\ldots\ldots,\frac{V}{2}-1. \end{cases} \tag{19}$$

Substituting (18) into (19) yields,

$$d_{q,m} = \begin{cases} \sum_{u=0}^{U-1} C_{u.V,m}\ , & q = 0, \\ \sum_{u=0}^{U-1} C_{u.V+\frac{V}{2},m}\ , & q = \frac{V}{2}, \\ \sum_{u=0}^{U-1} C_{u.V+q,m} + \sum_{u=0}^{U-1} C_{u.V+(V-q),m}, q = 1,2,\ldots\ldots,\frac{V}{2}-1 \end{cases} \tag{20}$$

It is worth noting that all operations before re-assembling are performed by HPM. Thus, the resulting signals are not equivalent to those obtained by DPM from the beginning. It is noted that the Sub-carrier Set Re-assembling block of the proposed time-domain architecture uses the time-domain repetition property (i.e., Property 5) in order to reduce the computational complexity. The sub-carrier set re-assembling operation is followed by the time-domain signal reversal process (see Fig.2). As with the complex conjugate operation, the system arbitrarily chooses whether or not to perform the reversal operation. The nth element of the resulting signal $e_{q,m}, q = 0,1,\ldots.,\frac{V}{2}$, therefore has the form

$$e_{q,m}[n] = d_{q,m}[n]\ or\ d_{q,m}[(-n)_N], q = 0,1,\ldots.,\frac{V}{2} \tag{20}$$

Finally, the m[th] candidate signal is obtained by adding all the $e_{q,m}[n]$ of the m[th] CSGB, to give

$$\tilde{X}_m = \sum_{q=0}^{V/2} e_{q,m} \tag{21}$$

Having generated M candidate signals, the signal with the lowest PAPR is selected for transmission. It should be noted that the proposed scheme requires various operations at the transmitter, but the related parameters can be stored at both the transmitter and receiver with code book. Therefore, the number of side information bits depends only on the number of candidate signals. If M candidate signals are generated, the scheme requires only $log_2[M]$ bits to transmit side information. In addition, the side information is assumed to be transmitted through the control channel, where channel coding is adopted to protect the side information from being erroneously detected.

VI. ANALYSIS OF COMPUTATIONAL COMPLEXITY

This section evaluates the computational complexities of the traditional SLM scheme and the proposed PAPR reduction scheme, respectively. The traditional SLM

scheme requires M N-point IFFTs to generate M different candidate signals, where each N-point IFFT requires $\frac{N}{2} \cdot log_2 N$ complex multiplications and $N \cdot log_2 N$ complex additions. Therefore, the total number of complex multiplications and complex additions are $\frac{MN}{2} \cdot log_2 MN$ and MN$\cdot log_2 MN$, respectively. For the PAPR reduction scheme proposed in this study, a total of S N-point IFFTs and M CSGBs are required to generate M candidate signals. The HPM partitioning method is adopted in order to maximize the PAPR diversity. Therefore, the sub-carriers are partitioned into S = U ·V sets. In the proposed architecture, most elements of the inputs to the IFFTs, i.e., X_s in (4), are zeros, and thus the IFFTs can be readily computed using the efficient algorithm proposed in [19]. It can be shown that the total number of complex multiplications and complex additions for S IFFT operations is therefore equal to $\frac{UN}{2} \cdot log_2 \frac{N}{UV} + N \cdot (U-1)$ and $UN \cdot log_2 UN$ respectively.

Regarding the computational complexity of each CSGB, Property 1 demonstrates that the time-domain equivalent operation on the right hand side of (8) does not require any complex multiplications or additions when the number of frequency-domain cyclic shifts belongs to $\left\{0, \frac{N}{4}, \frac{N}{2}, \frac{3N}{4}\right\}$ which implies that U = 2 or U = 4 should be adopted. Furthermore, Property 5 indicates that V = 2, 4 yields a significant reduction in the computational complexity. Therefore, four different combinations of U and V are considered in the remainder of this study, i.e., $(U,V) = \{(2,2),(2,4),(4,2),(4,4)\}$. However, increasing U and V increases the complexity of the PAPR reduction process. Furthermore, a series of preliminary simulations showed that there was no significant change in the PAPR reduction performance of the proposed scheme when using higher values of U and V as shown in Fig.3. Thus, in evaluating the performance of the proposed scheme, higher values of U and V were not considered. Since U = 2, 4 and V=2, 4 were adopted, the first three blocks of the CSGBs in the proposed scheme, i.e., the time-domain phase rotation, time-domain cyclic shifting, and time-domain complex conjugate operations, do not require any complex multiplications or additions, as indicated in Property1,2, and 3.

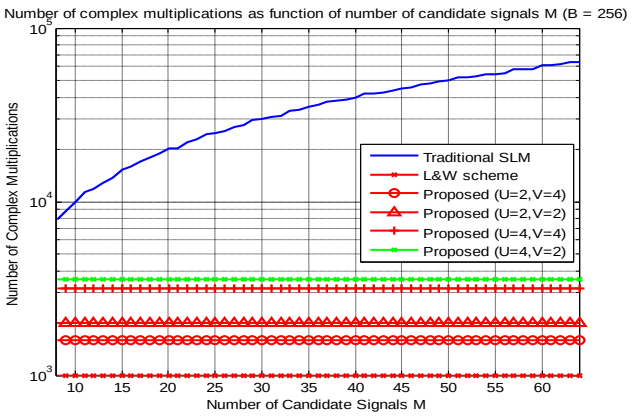

Fig.3. Number of complex multiplication as a number of candidate signals M (N=256).

SLM method and the method proposed by Li and Wang [15] for comparison purposes. It is seen that the number of complex multiplications in the traditional SLM scheme increases with an increasing number of candidate signals. However, in the proposed scheme and that of Li and Wang, the number of complex multiplications remains constant, irrespective of the number of candidate signals as shown in Fig.4. Of the three schemes, the method proposed in [15] requires the least number of complex multiplications, followed by the scheme proposed in this study with (U, V) = (2, 4) and (U, V) = (2, 2). By contrast, the proposed scheme with (U, V) = (2, 2) requires the minimal number of complex additions, followed by Li and Wang's method and the proposed scheme with (U, V) = (2, 4).

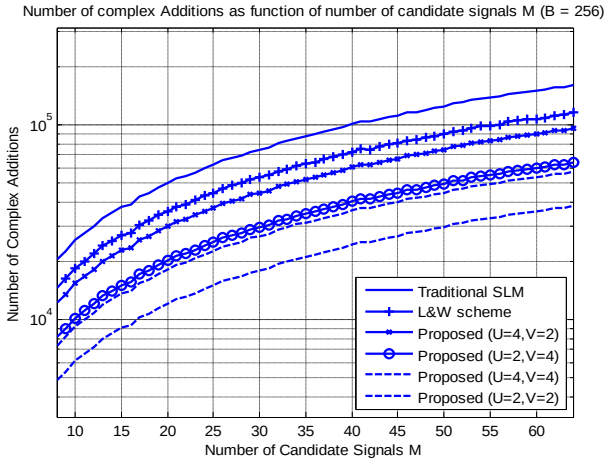

Fig.4. Number of complex additions as a function of number of candidate signals M (N=256).

VII. SIMULATION RESULTS

The PAPR reduction performance of the proposed scheme was evaluated by means of numerical simulations. Fig5 shows the PAPR reduction performance of the proposed scheme for an OFDM system with 256 sub-carriers and the 16-quadrature amplitude modulation (16-QAM) scheme. It can be seen that the PAPR reduction performance of the proposed scheme with (U, V) = (4, 4) is extremely close to that of the traditional SLM method.

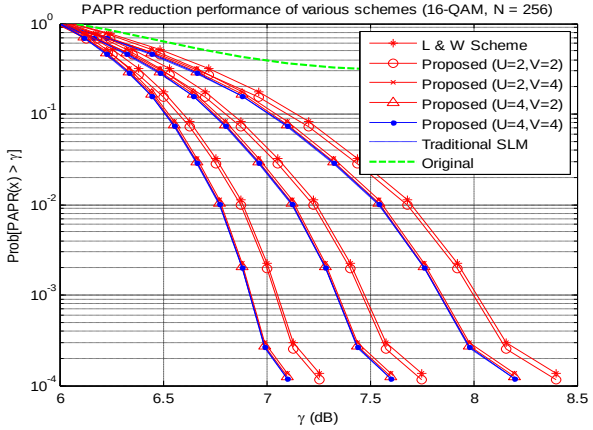

Fig.5. PAPR reduction performance of various schemes (16-QAM, N=256).

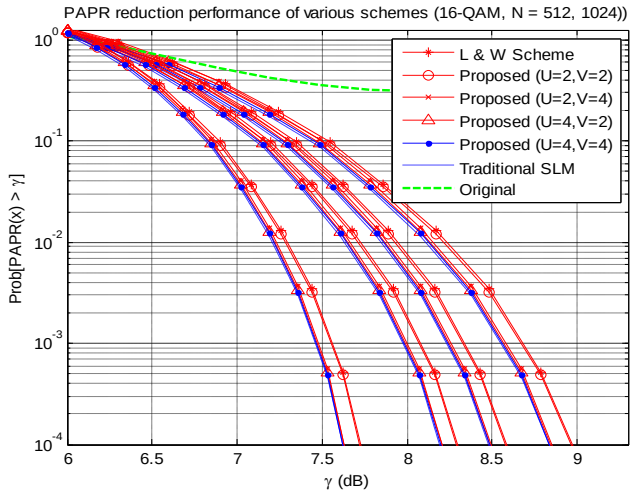

Fig.6. PAPR reduction performance of various schemes (16-QAM, N=512 and N=1024).

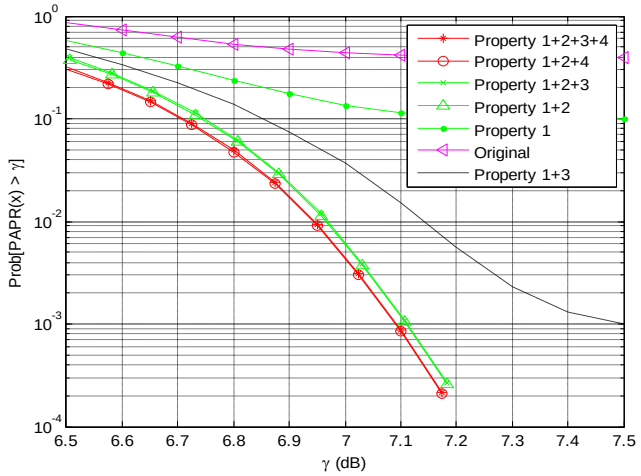

Fig.7.PAPR reduction performance of various combinations of frequency-domain operations (16-QAM, M = 32, N = 256, U = 4, V = 4).

From a detailed inspection, the performance loss of the proposed scheme relative to that of the traditional SLM method is found to be less than 0.001 dB for M = 32, U = 4, V = 4, and$Pr(PAPR(X) > \gamma = 10^{-4}$. Fig. 6 demonstrates the PAPR reduction performance for the cases of N = 512 and N = 1024. It can be seen that PAPR increases with the number of sub-carriers. However, the PAPR reduction performances of the proposed scheme are able to approach those of the traditional SLM scheme. A series of simulation experiments are conducted to investigate the PAPR reduction performance when various combinations of frequency-domain operations are performed. The results are demonstrated in Fig7, where the PAPR reduction performance basically increases with the number of extra frequency-domain operations. Fig.7 indicates that the improvement for Properties 1+2+3 is only marginal compared with Properties 1+2. Thus, the contribution of Property 3 (frequency-domain complex conjugate) is insignificant. However, the PAPR reduction performance when Properties 1+3 are adopted is better than when Property 1 alone is adopted. Therefore, the effect of equivalent frequency-domain operation in PAPR reduction depends on their order of operations. In addition, the PAPR reduction performance in general increases with the number of frequency-domain operations.

IX. CONCLUSION

Compared to the traditional SLM scheme, in which the candidate signals are generated using frequency-domain phase rotation only, a novel architecture is proposed in this study which additionally uses three operations namely, frequency domain cyclic shifting, complex conjugate and sub-carrier reversal operations can be performed to maximize the PAPR reduction performance of the candidate signals. In order to avoid the multiple-IFFT problem inherent in the traditional SLM method, the proposed scheme converts all four frequency-domain operations into time-domain equivalent operations. It has been shown that the computational complexity of the proposed approach can be minimized through an appropriate partitioning and reassembling of the sub-carriers in the OFDM system. In addition, the theoretical analysis results have shown that the number of complex multiplications and complex additions required in the proposed scheme for (U, V) = (4, 4) are 8.59% and 68.75%, respectively, of those required in the traditional SLM scheme. Furthermore, the simulation results have shown that the performance loss of the proposed scheme relative to that of the traditional SLM scheme is less than 0.001 dB for 16-QAM, M = 32, N = 256, U = 4, V = 4, and$Pr(PAPR(X) > \gamma) = 10^{-4}$. In other words, the proposed scheme closely approximates the PAPR reduction performance of the traditional SLM method, but with a significantly reduced computational complexity.

X. REFERENCES

[1]J.-C. Chen and C.-P. Li, "Tone reservation using near-optimal peak reduction tone set selection algorithm for PAPR reduction in OFDM systems," IEEE Signal Process. Lett., vol. 17, no. 11, pp. 933–936, Nov.2010.

[2]H. Li, T. Jiang, and Y. Zhou, "An improved tone reservation scheme with fast convergence for PAPR reduction in OFDM systems," IEEE Trans Broadcast., vol. 57, no. 4, pp. 902–906, Dec. 2011.

[3]S. Gazor and R. AliHemmati, "Tone reservation for OFDM systems by maximizing signal-to-distortion ratio," IEEE Trans. Wireless Commun., vol. 11, no. 2, pp. 762–770, Feb. 2012.

[4]T. Jiang, W. Xiang, P. C. Richardson, D. Qu, and G. Zhu, "On the nonlinear companding transform for reduction in PAPR of MCM signals," IEEE Trans. Wireless Commun., vol.6, no. 6, pp. 2017–2021, Jun. 2007.

[5]J.-C. Chen and C.-K. Wen, "PAPR reduction of OFDM signals using cross-entropy-based tone injection schemes," IEEE Signal Process. Lett., vol. 17, no. 8, pp. 727–730, Aug. 2010.

[6]B. S. Krongold and D. L. Jones, "PAR reduction in OFDM via active constellation extension," IEEE Trans. Broadcast., vol. 49, no. 3, pp. 258–268, Sep. 2003.

[7]K. Bae, J. G. Andrews, and E. J. Powers, "Adaptive active constellation extension algorithm for peak-to-average ratio reduction in OFDM," IEEE Commun. Lett., vol. 14, no. 1, pp. 39–41, Jan. 2010.

[8]P. Van Eetvelt, G. Wade, and M. Tomlinson, "Peak to average power reduction for OFDM schemes by selective scrambling," Elect. Lett., vol. 32, no. 21, pp. 1963–1964, Oct. 1996.

[9]A. D. S. Jayalath and C. Tellambura, "Reducing the peak-to-average power ratio of orthogonal frequency division multiplexing signal through bit or symbol interleaving," Electron. Lett., vol. 36, no. 13, pp. 1161– 1163, Jun. 2000.

[10]L. J. Cimini, Jr. and N. R. Sollenberger, "Peak-to-average power ratio reduction of an OFDM signal using partial transmit sequences," IEEE Commun. Lett., vol. 4, no. 3, pp. 86–88, Mar. 2000.

[11]J.-C. Chen, "Application of quantum-inspired evolutionary algorithm to reduce PAPR of an OFDM signal using partial transmit sequences technique," IEEE Trans. Broadcast., vol. 56, no. 1, pp. 110–113, Mar. 2010.

[12] T. Jiang and C. Li, "Simple alternative multi-sequences for PAPR reduction without side information in SFBC MIMO OFDM systems," IEEE Trans. Veh. Technol., vol. 61, no. 7, pp. 3311–3315, Sep. 2012.

[13] R. W. Ba¨uml, R. F. H. Fisher, and J. B. Huber, "Reducing the peak-toaverage power ratio of multicarrier modulation by selected mapping," Elect. Lett., vol. 32, no. 22, pp. 2056–2057, Oct. 1996.

[14] C.-L.Wang and Y. Ouyang, "Low-complexity selected mapping schemes for peak-to-average power ratio reduction in OFDM systems," IEEE Trans. Signal Process., vol. 53, no. 12, pp. 4652–4660, Dec. 2005.

[15] C.-P. Li, S.-H. Wang, and C.-L. Wang, "Novel low-complexity SLM schemes for PAPR reduction in OFDM systems," IEEE Trans. Signal Process., vol. 58, no. 5, pp. 2916–2921, May 2010.

[16] S.-H. Wang, J.-C. Sie, and C.-P. Li, "A low-complexity PAPR reduction scheme for OFDMA uplink systems," IEEE Trans. Wireless Commun., vol. 10, no. 4, pp. 1242–1251, Apr. 2011.

[17] W.-W. Hu, S.-H. Wang, and C.-P. Li, "Gaussian integer sequences with ideal periodic autocorrelation functions," IEEE Trans. Signal Process., vol. 60, no. 11, pp. 6074–6079, Nov. 2012.

[18] S.-H.Wang, K.-C. Lee, C.-P. Li, and H.-J. Li, "A low-complexity symbol interleaving-based PAPR reduction scheme for OFDM systems," in Proc. IEEE International Conference on Communications (IEEE ICC 2013), June 2013.